On The Effect of Preprocessing Techniques For Evapotranspiration Estimation Using Soft Computing Methods

Amin Amir-Ashayeri
Urmia University
Javad Behmanesh (j.behmanesh@urmia.ac.ir)
Urmia University
Vahid Reza Verdinezhad
Urmia University
Nasrin Fathollahzadeh Attar
Urmia University

Research Article

Keywords: Evapotranspiration, Pre-processing techniques, Penman-Monteith equation, Soft computing methods, Urmia Lake basin.

Posted Date: October 12th, 2021

DOI: https://doi.org/10.21203/rs.3.rs-711387/v1

On The Effect of Preprocessing Techniques for Evapotranspiration Estimation using Soft Computing Methods

Amin Amir-Ashayeri[1], Javad Behmanesh[1], Vahid Reza Verdinezhad[1], Nasrin Fathollahzadeh Attar[1]

[1]*Department of Water Engineering, Urmia University, Urmia, Iran*

Abstract

Implementing a reliable computational model for predicting the reference evapotranspiration (ET_0) process is essential for several agricultural and hydrological applications, especially for the rural water resource systems, water use allocations, utilization and demand assessments, and the management of irrigation systems. In this research, two artificial intelligence (AI) models, artificial neural network (ANN) and model tree (MT), were investigated for modelling ET_0. To validate model performance, five climatic stations such as Urmia, Mahabad, Takab, Khoy, and sardasht in West Azerbaijan Province of Iran. In the next step and to improve the model's accuracy, a novel preprocessing algorithm, ensemble empirical mode decomposition (EEMD), was coupled with those AI models to remove the trends or noise in the time series dataset. The extracted results indicated that the EEMD-MT model for all five stations outperformed other standalone and hybrid models.

Keywords: Evapotranspiration, Pre-processing techniques, Penman-Monteith equation, Soft computing methods, Urmia Lake basin.

Introduction

In most developing countries, the improper use of water is a substantial reason for water scarcity and water resources deprivation. In this regard, the Asian region contains semiarid and arid kinds of weather and a large chunk of its water use for several irrigation and agriculture activities (Jung et al., 2010; Marshall et al., 2012; Schüttemeyer et al., 2007). Mainly, the sustainability of agriculture, irrigation, and environmental aspects are related to the early Reference Evapotranspiration (ET_0) prediction. As a result, providing the need to obtain the accurate ET_0 prediction can optimize the operational projects, including the water use (Andam-Akorful et al., 2015; Sun et al., 2012). Besides, it is well known as one of the main components of the hydrological processes, which are critical for water resources planning and some watershed sustainability (Kisi, 2007; Rana and Katerji, 2000; Trajkovic, 2005).

In this matter, ET_0 can be specified using the manual empirical formulation by utilizing direct and expensive micrometeorological information (Abdullah et al., 2015), or the use of the Lysimeters that bring some challenges for the manufacture including both expenses and time for the research goals (Wright, 1988). Regarding approaches for the direct methods, the mathematical models by utilizing the estimated weather information (e.g., wind speed, humidity, solar radiation temperature) are developed, which are locally achieved at the meteorological stations of the watershed (Feng et al., 2017; Kisi, 2016). In ET_0 prediction, carious empirical methods are developed according to the Food and Agriculture Organization (FAO). In this regard, FAO proposes that a more accurate prediction could be obtained by considering the energy balance/aerodynamics. They confirmed the FAO Penman-Monteith (P-M) equation as the standard equation to estimate ET_0 (Penman, 1948). Nevertheless, many types of research indicated how other ET_0 models implement against the PMF-56 equation to obtain more

alternative equations via fewer data requirements, depending on fewer climatic data (Feng et al., 2017).

In recent decades, Artificial Intelligence (AI) models including artificial neural network (ANN) (Rezaie-Balf and Kisi, 2017; Zounemat-Kermani et al., 2018), gene expression programming (GEP) (Mohsenzadeh Karimi et al., 2018; Sarir et al., 2019), adaptive neuro-fuzzy inference system (ANFIS) (Shiri and Kisi, 2010; Keshtegar et al., 2017; Kisi et al., 2019), extreme learning machine (ELM) (Mouatadid and Adamowski, 2017; Rezaie-Balf and Kisi, 2017) model tree (MT) (Solomatine and Dulal, 2003; Solomatine and Xue, 2004; Bhattacharya and Solomatine, 2005; Rezaie-Balf et al., 2017), and support vector machine (SVM) (Kim et al., 2017; Azimi-pour et al., 2020) were developed to solve not only an extensive range of both water engineering and environmental problems. Nevertheless, developing robust and reliable methods remains a noticeable challenge to obtain accurate forecasting approaches.

As the time series data for the hydro-climatology parameters are obtained seasonal and nonlinear, employing the raw data directly to the model may not provide accurate and reliable results. In this regard, employing the data preprocessing method could improve the model's performance (Wu et al., 2010). In recent years, novel noise-assisted data analysis methods such as ensemble empirical mode decomposition (EEMD) and empirical mode decomposition (EMD)) have been proposed by Huang et al. (1998) and Wu and Huang (2009), respectively. Here, it is worthwhile to mention that the EEMD approach has been developed based on the traditional decomposition methods (e.g., wavelet and Fourier based decomposition), which was an empirical, intuitive and self-adaptive data processing tool. This technique is utilized for the nonstationary and nonlinear signal sequences (Huang and Wu, 2008; Hu et al., 2013). In this matter, to forecast runoff time series, various successful applications of the EMD/EEMD method

have were mentioned (Karthikeyan and Kumar, 2013; Kisi et al., 2014; Barge and Sharif, 2016). For example, Napolitano et al. (2011) investigated many ANN models to forecast daily streamflow using the EMD method. They revealed that the EMD method increased both the accuracy and reliability of ANN prediction. Moreover, Wang et al. (2013) implemented the EEMD method to decompose annual rainfall time series using an SVM model. They indicated that the proposed model increased efficiency and capability using the optimal SVM parameters for runoff forecasting. Rezaie-Balf et al. (2019) described the EEMD preprocessing algorithm to decompose runoff time series to improve their proposed models, namely multivariate adaptive regression spline (MARS) and EEMD based M5 model tree (M5Tree). They provided that hybrid EEMD-based models were a proper and robust tool to forecast single and multi-day-ahead river flows.

The main aim of the current research is to propose a novel preprocessing method to enhance the forecasting accuracy of DDAs. ANN and M5Tree techniques are investigated, and the forecasting accuracy is assessed by integrating these models with EEMD. Coupling EEMD with AI models, the specific models can be employed to raise both accuracy and reliability. By incorporating a long-term historical database of climatic predictor parameters as the input, the new hybrid system is tested in a real problem for predicting daily ET_0 over five regions (e.g., Urmia, Khoy, Mahabad, Takab, and Sardasht in Iran).

Method

The West Azerbaijan (WA) province, with a 39,487 km^2 area, is located northwest of Iran. WA is covered by the Zagros Mountains that extend from the northwest to the southeast. The water getting from the melting snow flows across the different valleys and conveys to Lake Urmia. The climate of this province is mainly affected using the rainy winds of the Atlantic Ocean and Mediterranean. Cold northern winds influence WA in the winter, which leads to vast snow. In this province, the temperature generally increases to 34 °C in July and falls to −16 °C in January. The average annual precipitation can vary from 300 mm (in the northern areas, which mainly is snow) and 870 mm (rainfall equivalent in the southern regions). Hence, in this study, five stations of WA province, namely Urmia, Mahabad, Khoy, Takab, and Sardasht, are considered to estimate ET. The map of the study area was demonstrated in Figure1. To obtain this aim, based on the recent researches, several parameters such as average temperature, average humidity, average air pressure, and maximum wind speed have been applied which their descriptive statistics (i.e., minimum (min), maximum (max), average, and standard deviation (SD)) are shown by Table 1.

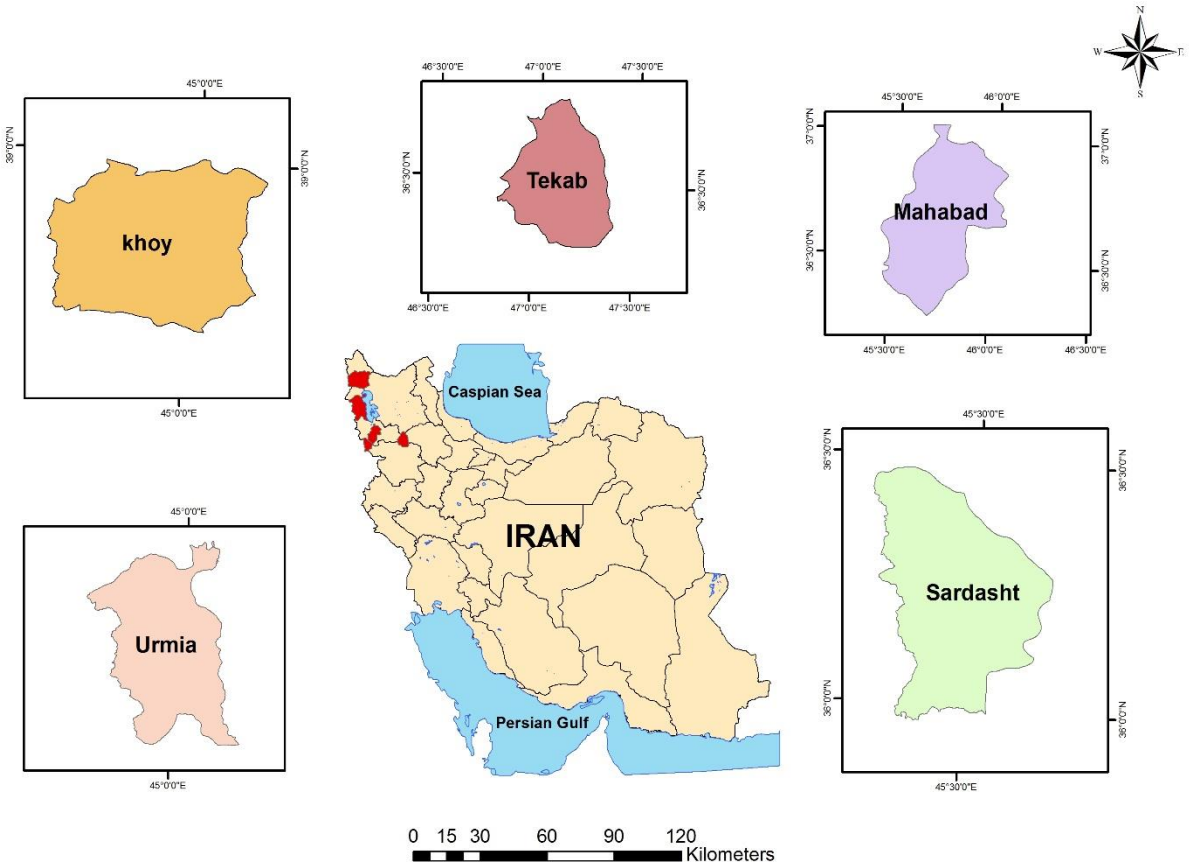

Figure1: The map of the study area

Table1: The mentioned stations with the parameters and their descriptive statistics

Station	Parameter	Average	Min	Max	SD
Urmia	Tmean	11.85	-12.9	30	9.58
	RHmean	58.32	15.37	99.5	15.84
	PV mean	8.15	1.37	19.58	3.51
	U2	5.33	0	40	2.46
	ET	3.94	0.27	14.43	2.68
Mahabad	Tmean	13.74	-13.5	34.5	9.87
	RHmean	49.78	10	97.5	19.00
	PV mean	7.31	1.14	16.76	2.73
	U2	6.57	0	37	3.70
	ET	5.04	0.18	17.45	3.56
Khoy	Tmean	13.1	-18.2	33.2	10.36
	RHmean	57	15.3	98	16.50

	PV mean	8.6	1.2	19.6	3.80
	U2	5.71	0	30	3.39
	ET	4.29	0.13	15.97	3.08
Takab	Tmean	10.4	-17.7	31.7	10.05
	RHmean	53	14.1	97.4	20.29
	PV mean	6.3	1	17	2.55
	U2	7.04	0	60	3.56
	ET	4.42	0.07	16.80	3.41
Sardasht	Tmean	14	-10	33.2	10.12
	RHmean	48.9	10.8	100	21.91
	PV mean	7.2	1.2	16.3	2.46
	U2	6.94	0	50	3.22
	ET	5.38	0.21	17.52	3.89

Allen et al. (1998) proposed the Penman-Monteith equation to calculate daily reference evapotranspiration (ET_o) (mm day^{-1}) as well as to prepare the reference data for both testing and training of proposed models in the current research. This empirical equation is computed as follow:

$$ET_0 = \frac{0.408\,(R_n - G) + \gamma \frac{900}{T+273} U_2 (e_s - e_a)}{\Delta + \gamma (1 + 0.34 U_2)} \quad (1)$$

where Δ means the slope of saturation vapour pressure versus the air temperature curve (kPa $^oC^{-1}$), R_n denotes the net radiation at the crop surface (MJ m^{-2} d^{-1}), G refers to the soil heat flux density at the soil surface (MJ m^{-2} d^{-1}), T denotes the mean daily air temperature (^oC), U_2 is the daily wind speed at 2 m height (m s^{-1}), e_s refers to the saturation vapour pressure (kPa), e_a means the actual vapour pressure (kPa), e_s-e_a is the saturation vapour pressure deficit (kPa), γ denotes the psychrometric constant (kPa $^oC^{-1}$).

Empirical mode decomposition (EEMD)

The ensemble empirical mode decomposition (EEMD) is well known as a particular type of mathematical function, which provides a nonstationary and nonlinear signal from the original data (Wu and Huang, 2009). In this way, the data preprocessing method is developed by improving the EMD method in order to decompose the time series signals (original data) into a small and finite number of oscillatory modes, according to the local characteristic time scale (Yeh et al., 2010). The oscillatory modes can be stated through the intrinsic mode functions (IMFs) components embedded in the data. The EMD is a self-adaptive time-frequency procedure, whereas the IMF provides a signal using a sum of zero-mean, which well-behaved slow and fast oscillation modes (Huang et al. 1998; Wu and Huang 2009). Overall, an IMF denotes a simple oscillatory mode, as compared to the simple harmonic function. According to the definition, a shifting process of the original time series (R-R) can be described briefly in the following (Yeh et al., 2010):

Step 1: Identify all extrema including local maxima and minima points of the considered time series y(t);

Step 2: Connect the obtained local maxima points in order to create an upper envelope $e_{max}(t)$ as well as all minima points to obtain a lower envelope $e_{min}(t)$ with spline interpolation, respectively;

Step 3: Calculate the mean m(t) between two envelopes using Eq. (2) :

$$m(t) = (e_{max}(t) + e_{min}(t))/2 \quad (2)$$

Step 4: Subtract the mean obtained from the data for generating an IMF as follows: $h(t) = y(t) - m(t)$.

Step 5: If h(t) satisfies two properties of IMF based on the predefined stopping criterion, h(t) is then defined as the first IMF [written as c1(t) and 1 is its index]; If h(t) is not an IMF, y(t) is then replaced with h(t) and iterate steps 1- 4 until h(t) meets the two conditions of IMF.

Step 6: The residue $r_1(t) = y(t)-c_1(t)$ is then treated as new data subjected to the same shifting process as described above for the next IMF from $r_1(t)$. In the final step, the shifting procedure will be stopped when the residue r(t) becomes a monotonic trend or contains one local maxima and minima point so that no more IMF could be extracted (Huang et al., 2003). The original signal y(t) can be reconstructed at the end of this shifting process using the sum of IMFs and residual by Eq. (3):

$$y(t) = \sum_{i=1}^{n} c_i(t) + r_n(t) \quad (3)$$

where $r_n(t)$ denotes the final residue, n means the number of IMFs, and ci(t) are approximately orthogonal to each other, along with all have zero means. Huang et al. (1998) and Huang et al. (2003) provided more information for the EMD method as well as the stopping criteria.

Therefore, the studies demonstrated that EMD is still unstable because of the mode of mixing drawback (Wu and Huang, 2009). In this way, the mode mixing can be described as either a component of a similar scale residing in different IMFs or a single IMF consisting of components of extensively disparate scales (Lei et al., 2009). To handle the problem of mode mixing in EMD, the EEMD is developed as a modified method. Regarding this argument, the whole time-frequency space would uniformly fill by adding the white noise.

167

168 ***Artificial Neural Network (ANN)***

169 By inspiring the mimic of the biological neural network in human brains, the Artificial neural
170 network (ANN) is developed as one of the computational methods (Agatonovic-Kustrin and
171 Beresford, 2000). ANN encompasses a set of nodes (neurons)that are placed in some layers. It
172 should be noted that each node in a layer obtains and then processes the weighted input from the
173 previous layer. Afterwards, in the following layer through links, the node transmits its output to
174 nodes. Each link is then allocated to a weight, indicating its connection power (Sudheer et al.,
175 2002). In this way, the weighted summation of inputs to a node is then converted to an output
176 based on a mathematical function such as logistic sigmoid, sigmoid, and hyperbolic tangent
177 sigmoid) or activation function, which determines the activation of the neuron. It should be noted
178 that these different artificial neurons combine with each other in order to process information as
179 well as to achieve the final output. A three-layered ANN, which encompasses layers *i*, *j*, and *k*
180 with weights W_{ij} and W_{jk}. The input *x* can be measured using the weighted sum of outputs of the
181 first layer and then allocated to each neuron of the second and third layers. For example, the y in
182 the second layer j can be measured using Eq. (4) (Kara et al., 2011):

$$y_{pj} = \sum_{i=1}^{I} W_{ij} O_{pi} + \theta_j \tag{4}$$

183 Whereθ_j, O_{pi} and W_{ij} denote the bias for neuron j, the ith output of the first layer, and the weights
184 between first and second layers, respectively. A nonlinear activation function is set to the y,
185 based on which the output $f(y)$ is then measured from each neuron in the second and third

186 layers (Rezaie-Balf et al., 2017). Nevertheless, the function of activation (namely, logistic
187 function) can be introduced in the form of Eq (5) as follows:

$$f(y) = \frac{1}{1 + e^{-y}} \tag{5}$$

188

189 ***Model Tree (M5Tree)***

190 M5 model tree (M5Tree) contains a state-of-art hierarchical algorithm to describe the
191 relationship between input-output parameters (Quinlan, 1992). In the following, the proposed
192 problem can be handled by dividing it into some sub-problems (i.e. sub-spaces) and constructing
193 a piecewise linear regression model for each sub-spaces. In classification trees (sub-domain), all
194 records are categorized by employing tree sorting from the roof to several leaves. Moreover,
195 according to the CART algorithm, the proposed model tree is formed, which considers the
196 continuous-class learning attributes. In addition, this algorithm has been developed as one of the
197 most capable approaches to state the meaningfully physical insight of a phenomenon (Talebi et
198 al., 2017).
199 During the M5Tree algorithm, the tree saves a linear model as a branch, which can predict the
200 class values of the portion of the dataset reaching the leaf. Concerning the specific attributes of
201 the data, the records will split into different portions (Solomatine and Xue, 2004). In the
202 following, the standard deviation is employed as a splitting criterion in order to specify the best
203 attribute for splitting the data set in each node. The tree can be achieved using the standard
204 deviation reduction (SDR), which maximizes the expected error reduction for each node as
205 follows:

$$SDR = sd(E) - \sum_i \frac{|E_i|}{|E|} sd(E_i) \quad (6)$$

Where E indicates a set of examples, which gains the leaf (node); however, E_i represents a subset of input data to the parent node. The methods of pruning are regarded for pruning back the overgrown trees in the next stage in order to deal with the overfitting problem as well as to obtain precise generalization. In this matter, in the following pruning procedure, the inner nodes (i.e. sub-trees) are then transformed into leaf nodes by replacing them with the linear regression functions. After pruning, the disjointed linear models of the neighbouring leaves are subjected to a smoothing process. Meanwhile, all the leaf models are then combined along the path back to the root for gaining the final model during the smoothing process, which could result in an accurate prediction (Solomatine & Dulal, 2003). Talebi et al. (2017) presented more details about the suggested model tree, its applications, and the model generating procedure.

Performance metrics

In the present study, the following performance measures (Eqs. 7-10) were applied, which are: The correlation coefficient (R), Nash-Sutcliffe Efficiency (NSE), Root Mean Square Error (RMSE), Ratio of RMSE to the standard deviation (RSD), [21,57–59]:

$$R = \frac{\sum_{i=1}^{N}(ET_{obs} - \overline{ET_{obs}}).\left(ET_{pre} - \overline{ET_{pre}}\right)}{\sqrt{\sum_{i=1}^{N}(ET_{obs} - \overline{ET_{obs}})^2 \sum_{i=1}^{N}\left(ET_{pre} - \overline{ET_{pre}}\right)^2}} \quad (7)$$

$$NSE = 1 - \frac{\sum_{i=1}^{N}\left(ET_{pre} - ET_{obs}\right)^2}{\sum_{i=1}^{N}(ET_{obs} - \overline{ET_{obs}})^2} \quad (8)$$

$$RMSE = \sqrt{\frac{1}{N}\sum_{i=1}^{N}\left(ET_{pre} - ET_{obs}\right)^2} \quad (9)$$

$$RSD = \frac{RSME}{\sum_{i=1}^{N}(ET_{obs} - \overline{ET_{obs}})} \quad (10)$$

In the above equations ET_{obs} and ET_{pre} denote the observed and predicted target variable values, respectively. $\overline{ET_{\mathrm{obs}}}$ and $\overline{ET_{\mathrm{pre}}}$ are the mean of observed and predicted target variable values, respectively.

Results and discussion

To establish the reliability of EEMD-MT, the results of three proposed approaches (ANN, MT, and EEMD-MT) for ET estimation are revealed. To assess the merits of the used AI techniques in the calibration and validation stages, several evaluation metrics, as expressed by Eqns. (7 - 10) are applied.

Urmia station

The predictive ability of the standalone and integrated MT model for ET prediction for both calibration and validation stages t has been seen concisely in Table 2. According to the evaluation metrics, for the Urima station, Romanenko performance with R=0.95 and RMSE=1.028 outperformed other predictive approaches such as ANN (R=0.87 and RMSE=1.612) in the calibration stage.

Table 2. Performance of proposed models at calibration and validation phases

	Calibration				
	Romanenko	Schendel	ANN	MT	EEMD-MT
R	0.95023	0.93951	0.87892	0.87707	0.87842

RMSE	1.0289	1.7242	1.6121	1.738	1.7361
RSD	0.33742	0.56542	0.52865	0.56995	0.56932
NSE	0.88612	0.68024	0.72047	0.67509	0.67582
			Validation		
R	0.95413292	0.942316	0.977396	0.984383	0.98913
RMSE	1.21099704	2.153919	0.704822	0.581216	0.487416
RSD	0.3791303	0.674334	0.220661	0.181963	0.152597
NSE	0.85618146	0.545025	0.951282	0.966871	0.976701

Despite the acceptable accuracy of empirical approaches in the calibration stage, for validation sate, the inability of these approaches compared to AI models was obvious. On the other hand, the integration of EEMD with the MT model leads to improve model performances by providing the lowest RMSE (0.487) and RSD (0.152) in ET estimation. After that, the MT model with higher RMSE and RSD (19.24%) than EEMD-MT provided better results than others.

Additionally, for achieving a particular conception of the model's abilities, the scatter plots of the observed and predicted validation dataset were illustrated in Figure 2. The greatest R2 indicated the good agreements between observed and estimated ET values that the EEMD-MT model roughly had a better performance than other methods. The peak ET estimated values versus observed ones in calibration and validation stages were shown in Figure 3. Among the used methods, the difference between observed and forecasted ET by the Schendel equation is the largest.

253

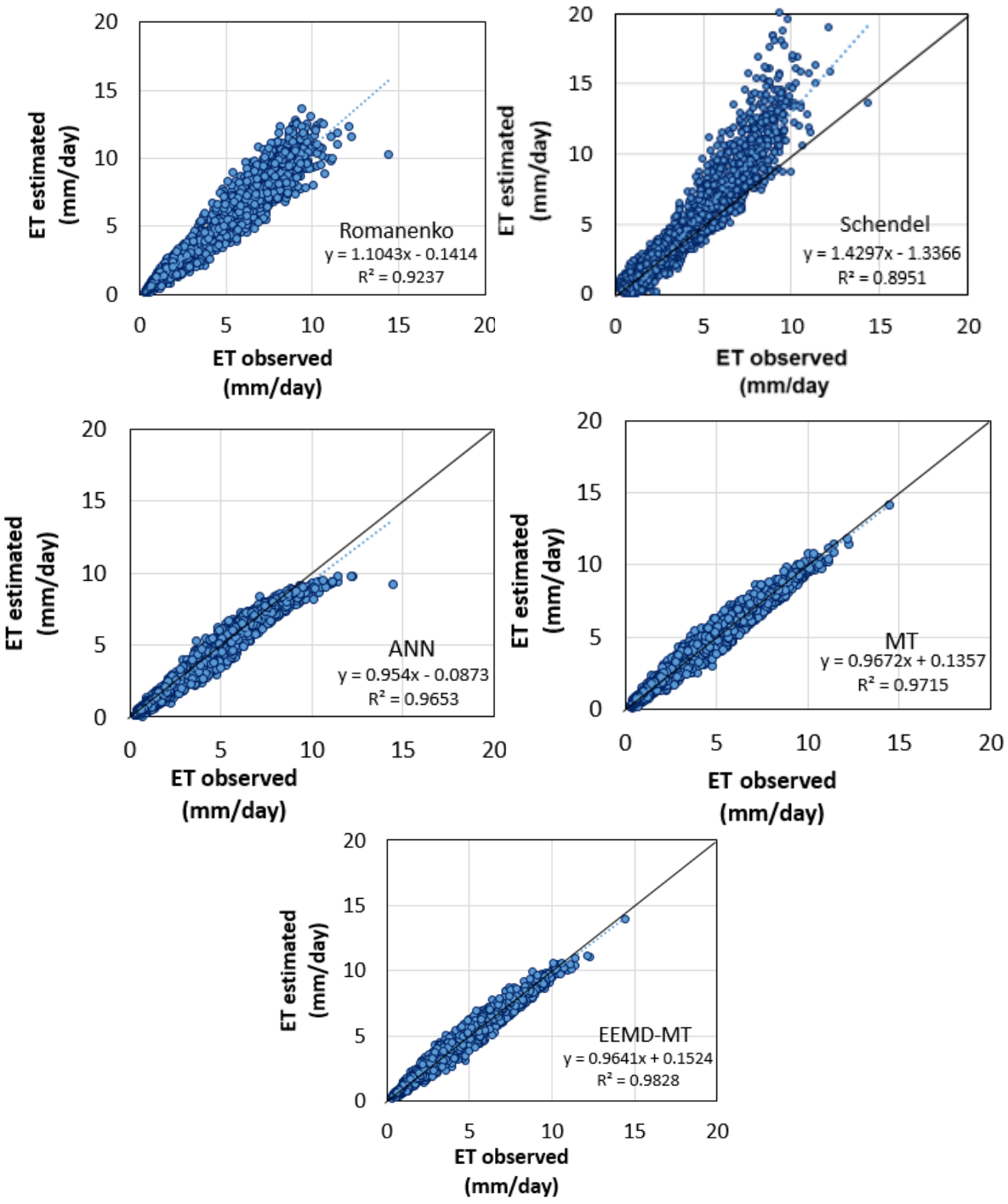

254

255

256 **Figure 2.** Scatter plots of estimated versus observed ET values for the validation phase

257

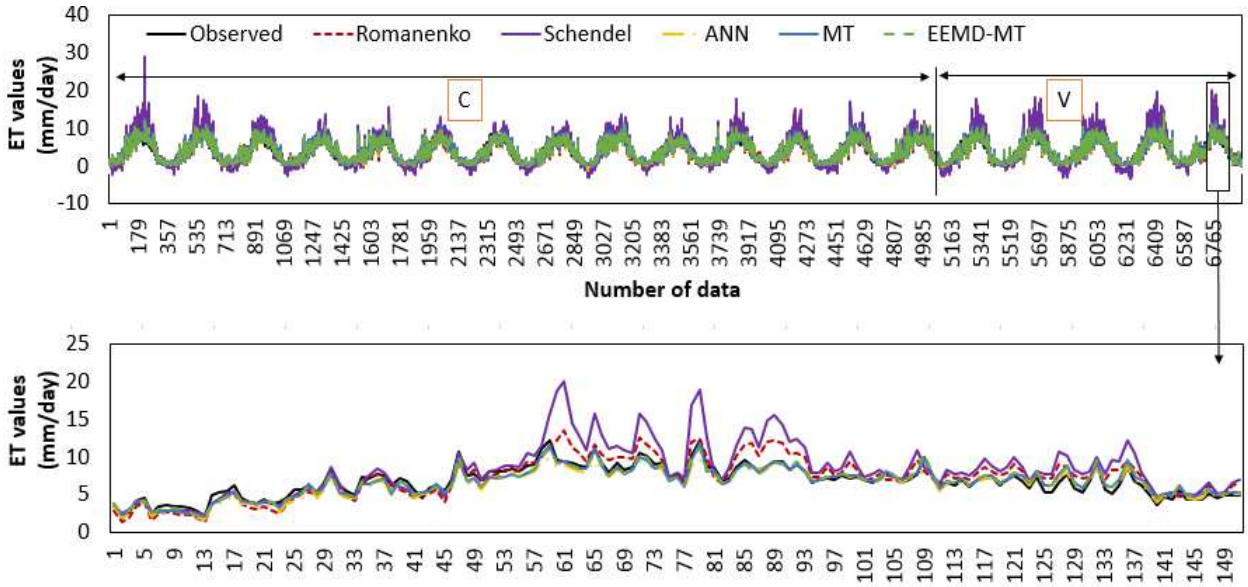

Figure 3. time series plot of estimated versus observed ET values for the calibration and validation phases

Mahabad station

The evaluation of the trend of model performances for ET prediction at calibration dataset has been performed. Error metric values revealed that AI models had remarkable differences with empirical models to estimate ET at calibration and validation stages (Table 3). At the calibration stage, EEMD-MT with the maximum values of NSE (0.983) and R (0.99) have permissible accuracy comparing to other alternative methods such as Schendel (R=0.95 and NSE=0.865) as well as ANN (R=0.98 and NSE=0.967).

Table 3. Performance of proposed models at calibration and validation phases

	Calibration				
	Romanenko	Schendel	ANN	MT	EEMD-MT
R	0.95551	0.9186	0.98723	0.991	0.99163
RMSE	1.2491	3.4912	0.60974	0.4562	0.43984
RSD	0.36657	1.0246	0.17895	0.13389	0.12908
NSE	0.8656	-0.04999	0.96797	0.98207	0.9833

Validation					
R	0.933277	0.891135	0.928571	0.933053	0.95821
RMSE	1.682468	5.40617	1.752436	1.587255	1.2751
RSD	0.424	1.362414	0.441633	0.400006	0.321339
NSE	0.820125	-0.85719	0.804853	0.839908	0.896685

Likewise, as seen in Table 3, the EEMD-MT technique could create the lowest accuracy (RMSE=1.275 and RSD (0.321) for ET estimating in the validation stage. Besides, the significantly higher RMSE percentage (323.98%) of the Schendel equation comparing to EEMD-MT illustrated that the Schendel equation was not a suitable model to predict ET.

Additionally, scatter plots and time series of estimated against the observed ET were illustrated by Figures 4 & 5. In terms of scatter plots, the slope of the ET values provided by the EEMD-MT method was closest to the ideal line, and a huge number of ET forecasted values were underestimated, and the hybrid method (EEMD-MT) had the best performance than other models, especially Schendel equation for determining the peak values.

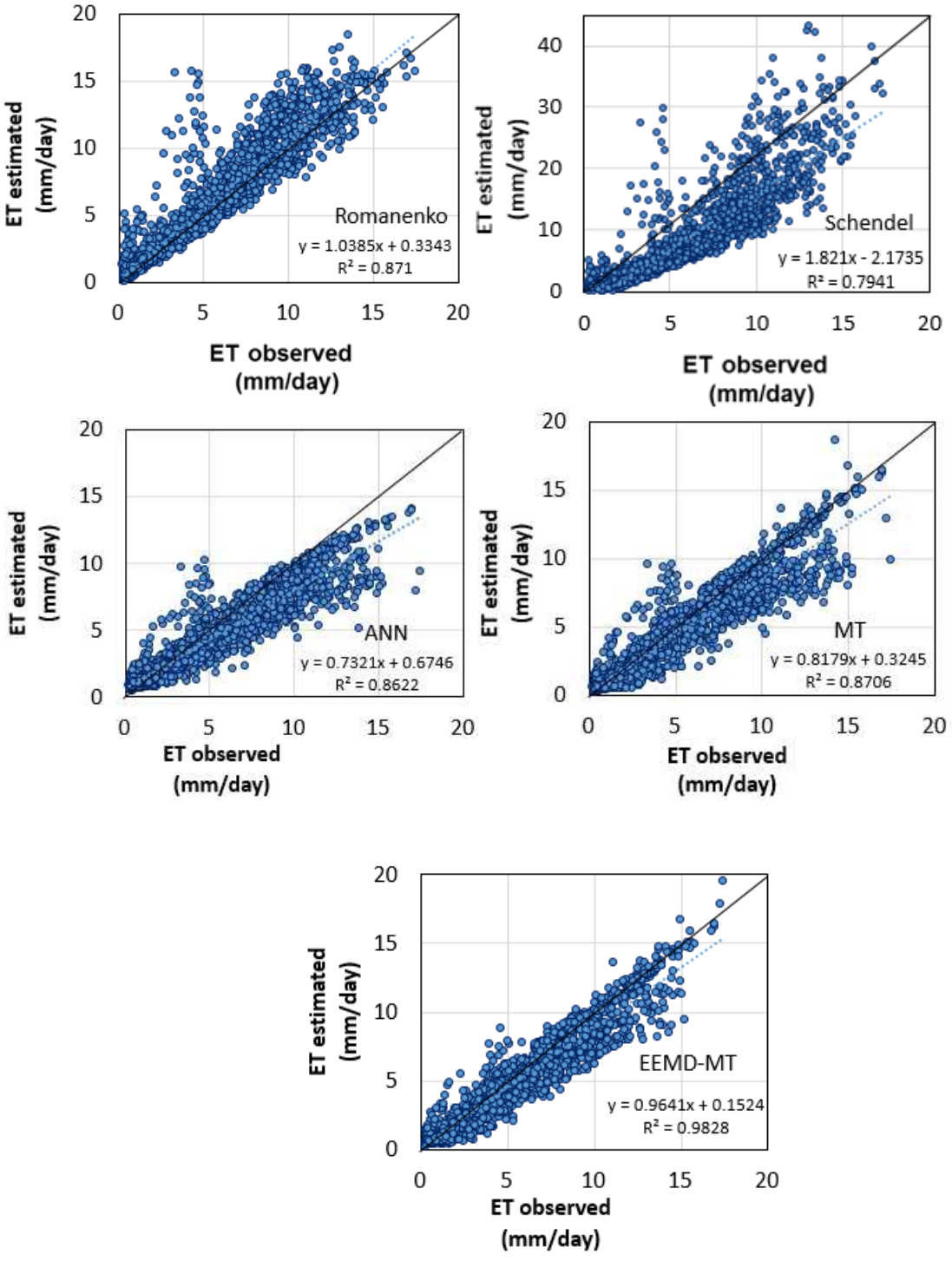

Figure 4. Scatter plots of estimated versus observed ET values for the validation phase

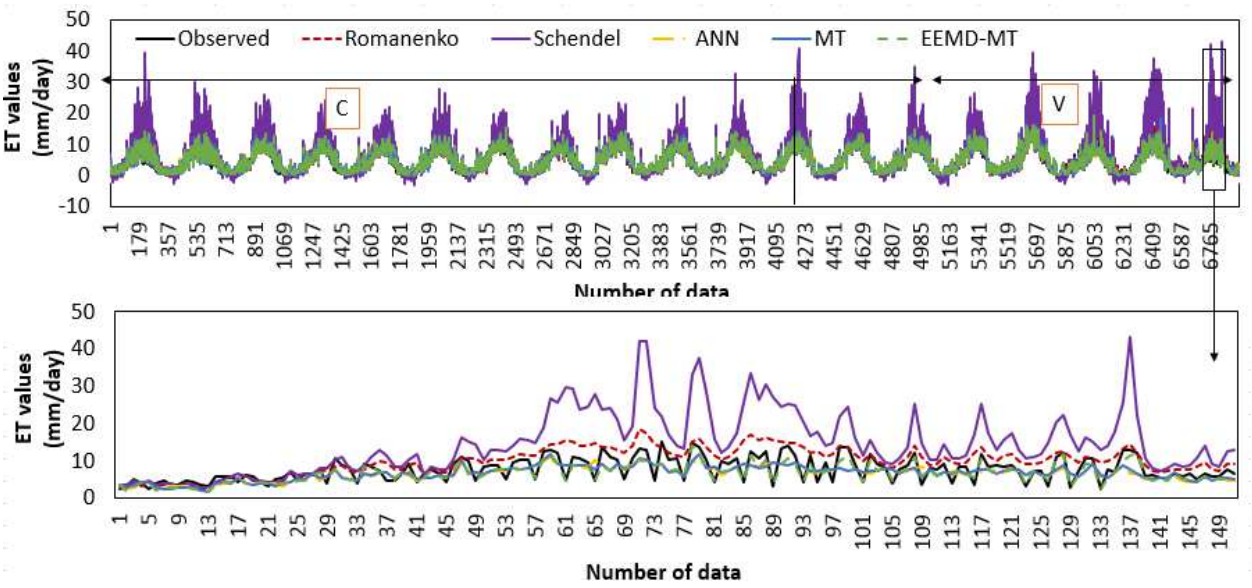

Figure 5. Time series plot of estimated versus observed ET values for the calibration and validation phases

Khoy station

Regarding Table 4, the equation provided by Romanenko achieved preferable precision (i.e., generally largest Rand lowest RMSE) in comparison with AI methods such as MT (R=0.87 and RMSE=1.738) and ANN (R=0.87 and RMSE=1.612) in the calibration stage. Besides, despite the acceptable R computed value of the Schendel equation (0.93), other evaluation metrics Indicated the inability of the model for ET prediction.

In the case of the validation stage, the criteria metrics in terms of RSD (0.152) and NSE (0.976) given by EEMD-MT was superior to other approaches such as the Schendel equation with higher RSD (343.42%) and lower NSE (44.15%) which stood at the last rank which indicates that EEMD has remarkably influence on increasing the AI accuracies for ET predicting.

Table 4. Performance of proposed models at calibration and validation phases

	Romanenko	Schendel	ANN	MT	EEMD-MT
Calibration					
R	0.95023	0.93951	0.87892	0.87707	0.87842
RMSE	1.0289	1.7242	1.6121	1.738	1.7361
RSD	0.33742	0.56542	0.52865	0.56995	0.56932
NSE	0.88612	0.68024	0.72047	0.67509	0.67582
Validation					
R	0.954133	0.942316	0.977396	0.984383	0.98913
RMSE	1.210997	2.153919	0.704822	0.581216	0.487416
RSD	0.37913	0.674334	0.220661	0.181963	0.152597
NSE	0.856181	0.545025	0.951282	0.966871	0.976701

The time series and scatter plots of forecasted *vs.* observed values of ET for the proposed approaches (Figs. 8 & 9) indicated that the model obtained by integration of EEMD and MT gave fewer scattered estimates are comparing with ANN MT, Schendel as well as Romanenko methods. Besides, the differences of one of the maximum observed ET values (13.00) and corresponding predicted values by the proposed methods, EEMD-MT, MT, ANN, Schendel, and Romanenko, were about 2.07%, 2.10%, 5.20%, 65.06%, and 17.61%, respectively

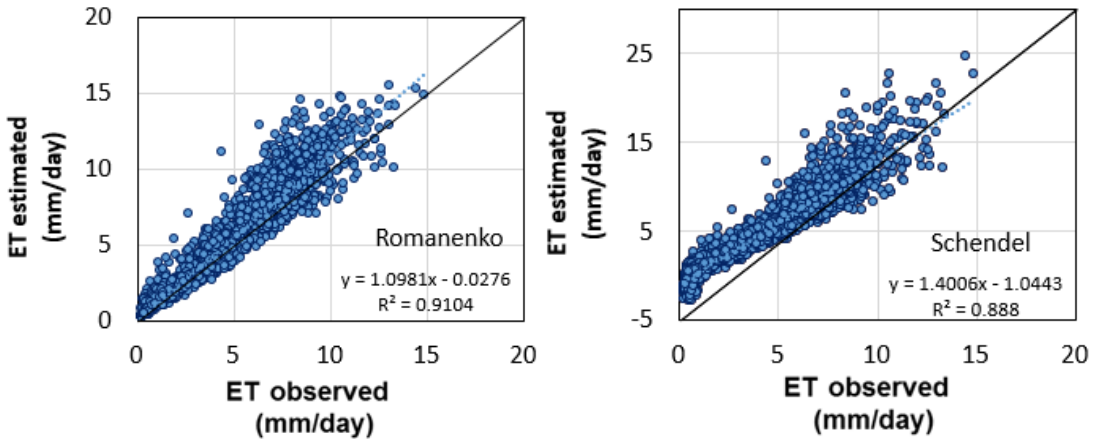

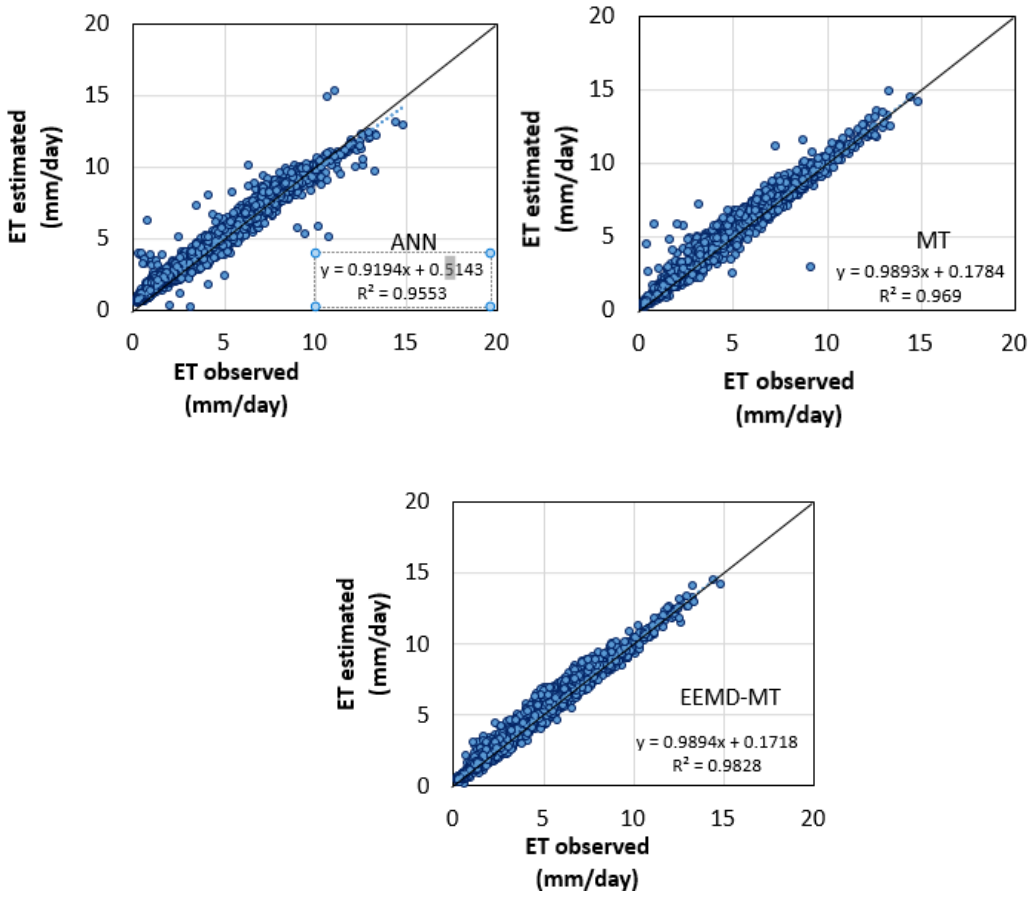

Figure 6. Scatter plots of estimated versus observed ET values for the validation phase

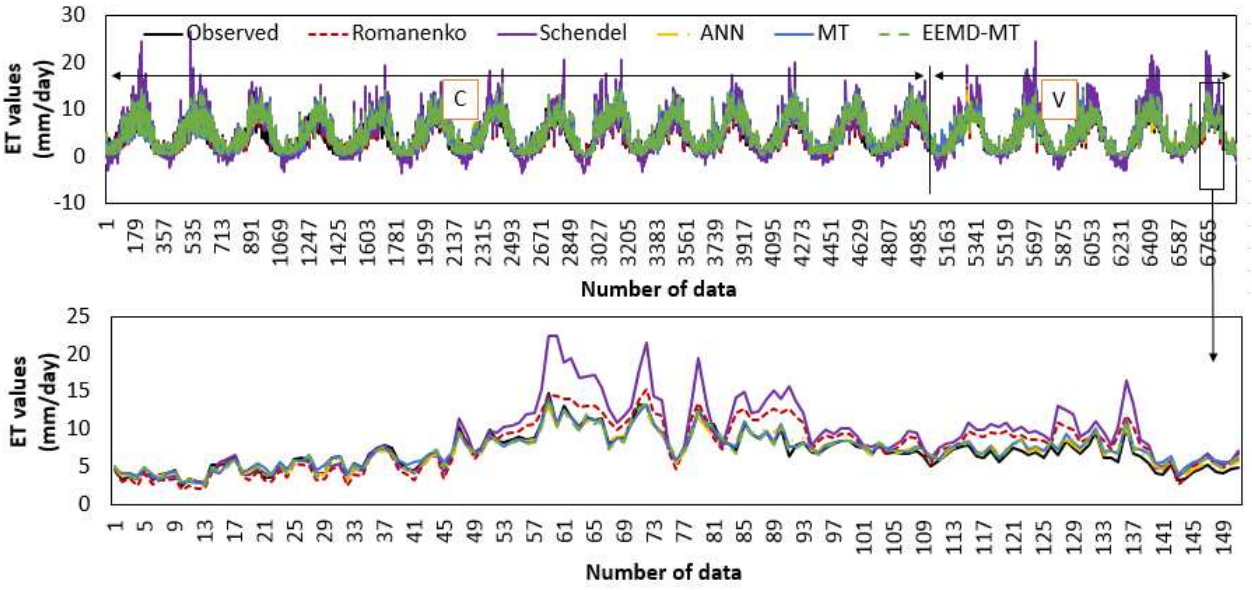

Figure 7. Time series plot of estimated versus observed ET values for the calibration and validation phases

Takab station

Similar to Urmia and Khoy stations, according to the comparison accuracy of the proposed models at the calibration stage (Table 5), it is explicit that in ET estimating, the best-forecasted ET values (regarding the observed values) were yielded using the Romanenko equation with respect to the statistical parameters (highest R =0.96, lowest RSD =0.266 and RMSE =0.885) than inferior findings for ANN (R=0.91, RMSE=1.384, and RSD=0.416) which has the best performance than MT, EEMD-MT, and Schendel methods.

Table 5. Performance of proposed models at calibration and validation phases

	Romanenko	Schendel	ANN	MT	EEMD-MT
Calibration					
R	0.96794	0.93224	0.91933	0.91459	0.91609
RMSE	0.88515	2.783	1.384	1.4795	1.4736
RSD	0.26667	0.83843	0.41696	0.44574	0.44396
NSE	0.92887	0.29689	0.82611	0.80128	0.80286
Validation					
R	0.966954	0.94396	0.988246	0.988353	0.988812
RMSE	1.035959	3.198179	0.631181	0.56853	0.557113
RSD	0.282745	0.872881	0.172269	0.155169	0.152053
NSE	0.920012	0.237662	0.970307	0.975909	0.976867

At the validation stage, the evaluation metrics in terms of RSD (0.152) and NSE (0.976) provided by EEMD-MT had the best results than other methods such as ANN (RSD=0.220 and NSE=0.951) and Schendel equation (RSD=0.674 and NSE=0.545). Moreover, Although the Romanenko equation stood at the first rank at the calibration stage, this model with higher RSD (85.52%) and lower NSE (5.73%) had lower accuracy EEMD-MT in ET forecasting.

Scatter plots of predicted vs. validation observed ET values had been shown in Figure 8. Most noticeably, ET predicted values were over-estimated, and for AI models, the slopes are close to the ideal value of one. Besides, Romanenko and Schendel equations were shown not to forecast ET as well as AI models. Figure 9 also illustrated the time series of forecasted and observed ET values for the entire calibration and validation dataset. MT and EEMD-MT proved to be the potential techniques to forecast ET, while the Schendel equation underestimated the maximum ET values, illustrating the minimum ability of this method to predict ET.

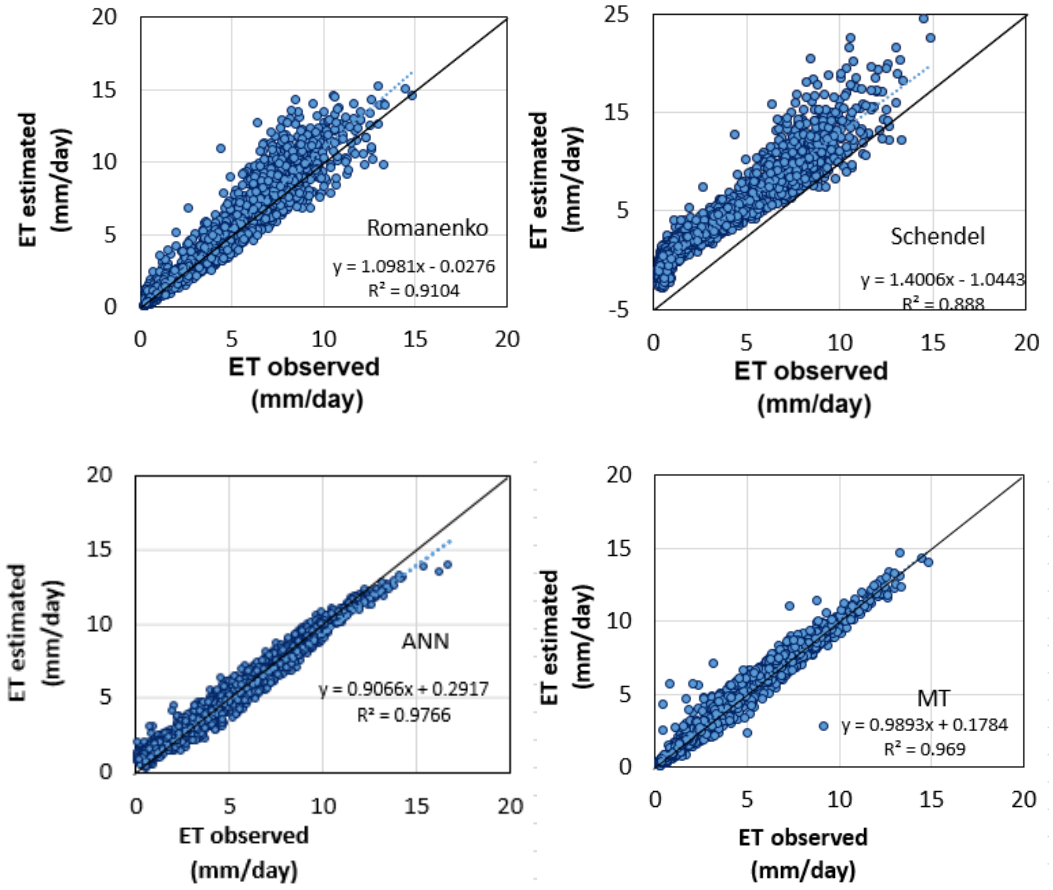

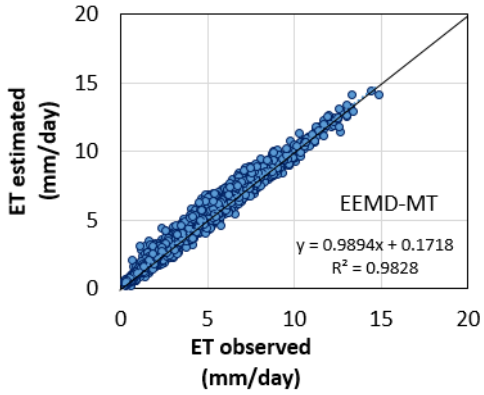

Figure 8. Scatter plots of estimated versus observed ET values for the validation phase

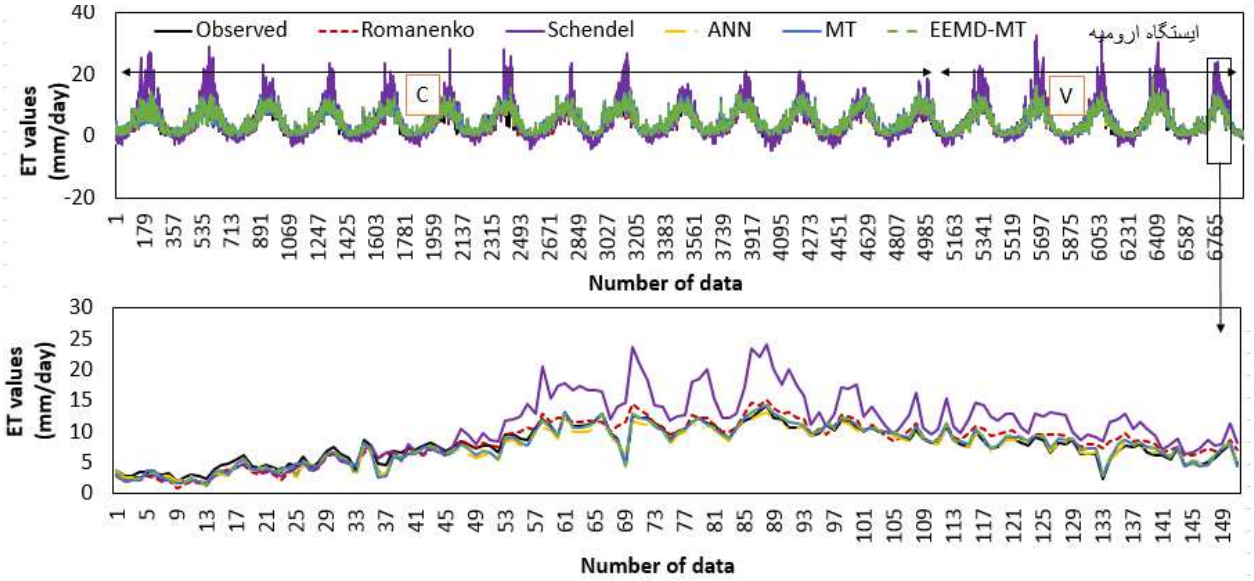

Figure 9. time series plot of estimated versus observed ET values for the calibration and validation phases

Sardasht station

Similar to other stations, evaluation criteria R, RMSE, NSE, and RSD were applied to ET forecasting for both calibration and validation stages at the Sardasht station, and the results were demonstrated in Table 6. In terms of ET predicting in the calibration stage, integrating MT and

EEMD (EEMD-MT) with the lowest error (RSD=0.114; RMSE=0.448) had high superiority compared with all other models. Whereas, Schendel equation generated poor performance for ET forecasting in terms of RSD (1.09) and RMSE (4.284) (Table 6).

Table 6. Performance of proposed models at calibration and validation phases

	Romanenko	Schendel	ANN	MT	EEMD-MT
Calibration					
R	0.968	0.92561	0.99119	0.99317	0.99344
RMSE	1.1951	4.2848	0.5826	0.45751	0.448
RSD	0.30471	1.0925	0.14854	0.11665	0.11438
NSE	0.90713	-0.19368	0.97793	0.98639	0.986
Validation					
R	0.972137	0.936437	0.993728	0.995661	0.99576
RMSE	1.401487	4.650306	0.478047	0.35958	0.356021
RSD	0.368798	1.223716	0.125797	0.094623	0.093686
NSE	0.863913	-0.49831	0.984166	0.991042	0.991218

Similar to the results of the calibration stage, the EEMD-MT technique gave the highest ET estimating accuracy (R= 0.99; RMSE= 0.356 and RSD=0.09; Table 6) for the validation dataset. Evaluation of EEMD efficiency in ET forecasting also indicated that integrating this preprocessing approach can enhance the MT method. As seen in Table 6 about the Schendel equation, this model could not predict ET values with the highest error in terms of RMSE of 4.650 and RSD of 1.223.

Similar to other stations, the goodness-of-fit and Pearson's correlation coefficients (R) between predicted and observed and ET values at the validation stage were shown as a scatterplot in Figure 10. As shown in this Figure, AI models, particularly EEMD-MT, skillfully forecasted the ET values; thereby, they were considered as the suitable model for the Sardasht station. The prediction outcome of observed and estimated ET at the Sardasht station was similar to that of the previous stations. On the other hand, it is noteworthy that the proposed EEMD-MT

reveals the most accurate findings compared to other models with respect to the general tendency and forecasting abilities of the ET peak values (Figure 11).

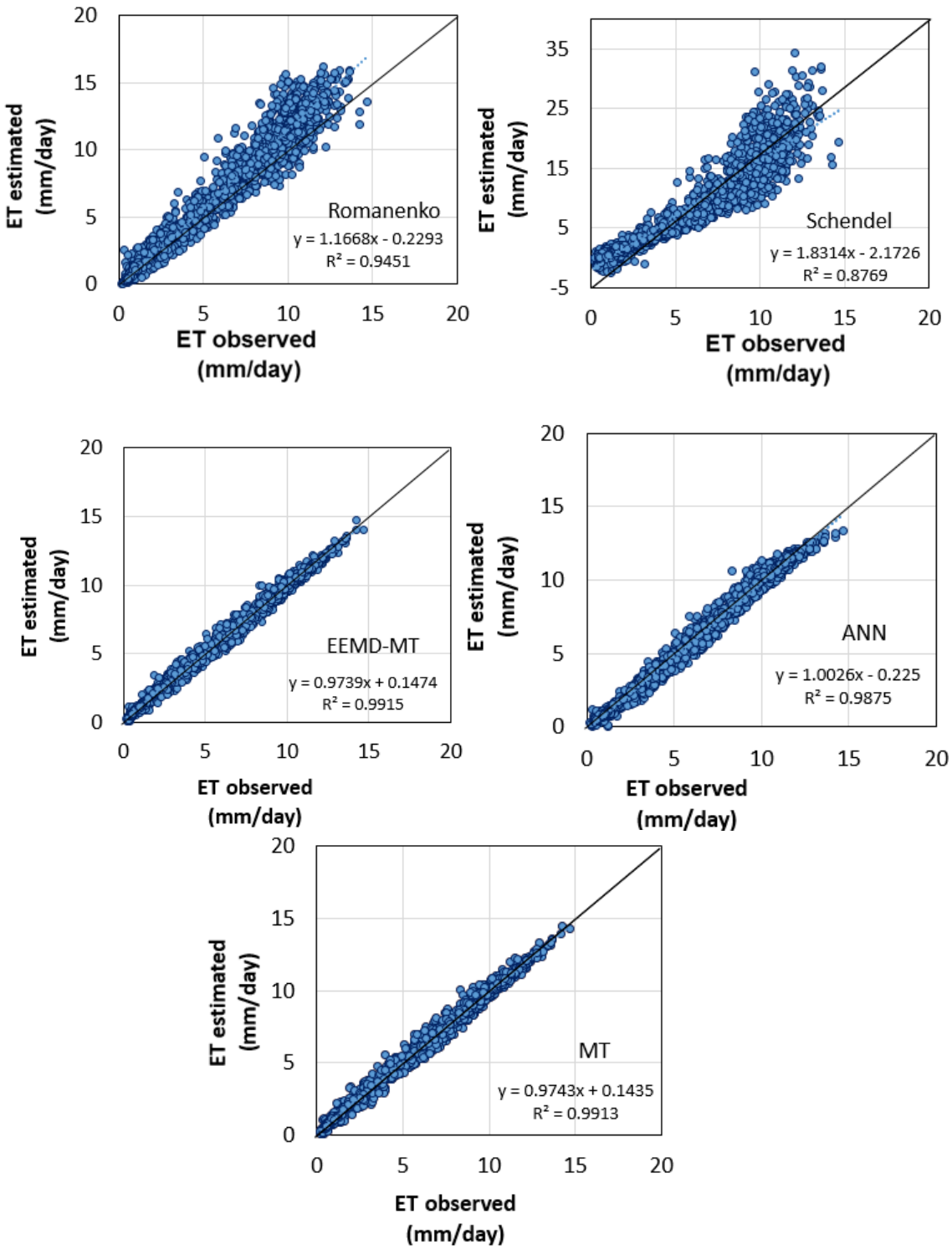

Figure 10. Scatter plots of estimated versus observed ET values for the validation phase

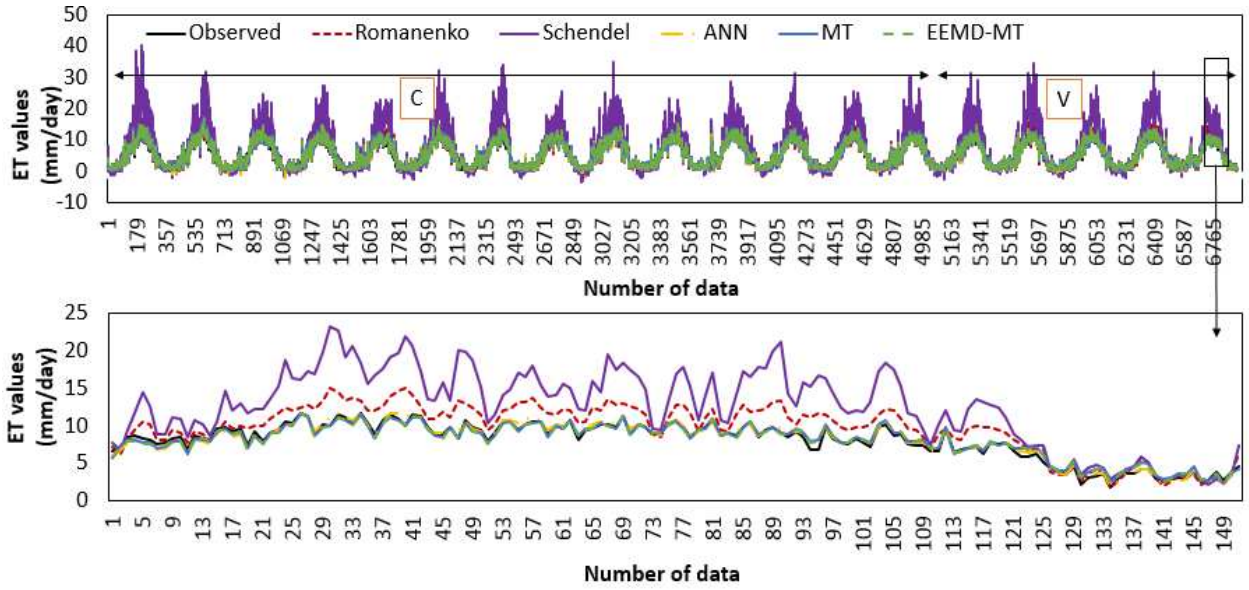

Figure 11. Time series plot of estimated versus observed ET values for the calibration and validation phases

Conclusion

An accurate prediction of actual evapotranspiration is essential for the estimation of irrigation needs and, more generally, for the careful management of water resources. If experimental data are available, AI algorithms represent a powerful tool able to provide accurate predictions. In this study, two AI models were built to predict actual evapotranspiration in West Azerbaijan Province, with a hot-summer Mediterranean climate. To predict ET0, ANN, and MT models using four input variables, average temperature, average humidity, average air pressure, and maximum wind speed, were constructed.

Comparing the results of the standalone and hybrid models revealed that the EEMD data-decomposition technique has a significant influence on models' accuracy. This approach can successfully decompose the dataset and solve the nonstationary associated with time-series records. At all gauging stations, the predicted ET_0 records were investigated in terms of evaluation metrics. Performance of EEMD-MT and EEMD-ANN indicated the computed values of the R and NSE increased compared with standalone ANN and MT models. Performances of empirical equations indicated that Romanenko provided a lower error of ET_0 predictions in terms of RMSE and RSD than Schendel. In the future, the proposed method can be tested to generate ET_o forecasts daily and weekly and at longer lead times timescales. More efforts can be devoted to investigating the use of ensemble ET_o predictions in agriculture and other areas.

References

Abdullah, S. S., Malek, M. A., Abdullah, N. S., Kisi, O., & Yap, K. S. (2015). Extreme learning machines: a new approach for prediction of reference evapotranspiration. *Journal of Hydrology*, *527*, 184-195.

Agatonovic-Kustrin, S., & Beresford, R. (2000). Basic concepts of artificial neural network (ANN) modeling and its application in pharmaceutical research. *Journal of pharmaceutical and biomedical analysis*, *22*(5), 717-727.

Allen, R. G., Pereira, L. S., Raes, D., & Smith, M. (1998). Crop evapotranspiration-Guidelines for computing crop water requirements-FAO Irrigation and drainage paper 56. *Fao, Rome*, *300*(9), D05109.

Andam-Akorful, S. A., Ferreira, V. G., Awange, J. L., Forootan, E., & He, X. F. (2015). Multi-model and multi-sensor estimations of evapotranspiration over the Volta Basin, West Africa. *International Journal of Climatology*, *35*(10), 3132-3145.

Azimi-Pour, M., Eskandari-Naddaf, H., & Pakzad, A. (2020). Linear and nonlinear SVM prediction for fresh properties and compressive strength of high volume fly ash self-compacting concrete. *Construction and Building Materials*, *230*, 117021.

Barge, J. T., & Sharif, H. O. (2016). An ensemble empirical mode decomposition, self-organizing map, and linear genetic programming approach for forecasting river streamflow. *Water*, *8*(6), 247.

Bhattacharya, B., & Solomatine, D. P. (2005). Neural networks and M5 model trees in modelling water level–discharge relationship. *Neurocomputing*, *63*, 381-396.

Jung, M., Reichstein, M., Ciais, P., Seneviratne, S. I., Sheffield, J., Goulden, M. L., ... & Dolman, A. J. (2010). Recent decline in the global land evapotranspiration trend due to limited moisture supply. *Nature*, *467*(7318), 951-954.

Feng, Y., Peng, Y., Cui, N., Gong, D., & Zhang, K. (2017). Modeling reference evapotranspiration using extreme learning machine and generalized regression neural network only with temperature data. *Computers and Electronics in Agriculture*, *136*, 71-78.

Feng, Y., Cui, N., Gong, D., Zhang, Q., & Zhao, L. (2017). Evaluation of random forests and generalized regression neural networks for daily reference evapotranspiration modelling. *Agricultural Water Management*, *193*, 163-173.

Hu, J., Wang, J., & Zeng, G. (2013). A hybrid forecasting approach applied to wind speed time series. *Renewable Energy*, *60*, 185-194.

Huang, N. E., Wu, M. L. C., Long, S. R., Shen, S. S., Qu, W., Gloersen, P., & Fan, K. L. (2003). A confidence limit for the empirical mode decomposition and Hilbert spectral analysis. *Proceedings of the Royal Society of London. Series A: Mathematical, Physical and Engineering Sciences*, *459*(2037), 2317-2345.

Huang, N. E., & Wu, Z. (2008). A review on Hilbert-Huang transform: Method and its applications to geophysical studies. *Reviews of geophysics*, *46*(2).

Kara, Y., Boyacioglu, M. A., & Baykan, Ö. K. (2011). Predicting direction of stock price index movement using artificial neural networks and support vector machines: The sample of the Istanbul Stock Exchange. *Expert systems with Applications*, *38*(5), 5311-5319.

Karthikeyan, L., & Kumar, D. N. (2013). Predictability of nonstationary time series using wavelet and EMD based ARMA models. *Journal of hydrology*, *502*, 103-119.

Kim, S., Seo, Y., Rezaie-Balf, M., Kisi, O., Ghorbani, M. A., & Singh, V. P. (2019). Evaluation of daily solar radiation flux using soft computing approaches based on different meteorological information: peninsula vs continent. *Theoretical and Applied Climatology*, *137*(1-2), 693-712.

Kisi, O. (2007). Evapotranspiration modelling from climatic data using a neural computing technique. *Hydrological Processes: An International Journal*, *21*(14), 1925-1934.

Kisi, O. (2016). Modeling reference evapotranspiration using three different heuristic regression approaches. *Agricultural Water Management*, *169*, 162-172.

Keshtegar, B., Kisi, O., Arab, H. G., & Zounemat-Kermani, M. (2018). Subset modeling basis ANFIS for prediction of the reference evapotranspiration. *Water resources management*, *32*(3), 1101-1116.

Kisi, O., Gorgij, A. D., Zounemat-Kermani, M., Mahdavi-Meymand, A., & Kim, S. (2019). Drought forecasting using novel heuristic methods in a semiarid environment. *Journal of Hydrology*, *578*, 124053.

Lei, Y., He, Z., & Zi, Y. (2009). Application of the EEMD method to rotor fault diagnosis of rotating machinery. *Mechanical Systems and Signal Processing*, *23*(4), 1327-1338.

Marshall, M., Funk, C., & Michaelsen, J. (2012). Examining evapotranspiration trends in Africa. *Climate dynamics*, *38*(9-10), 1849-1865.

Sun, S., Chen, H., Wang, G., Li, J., Mu, M., Yan, G., ... & Zhu, S. (2016). Shift in potential evapotranspiration and its implications for dryness/wetness over Southwest China. *Journal of Geophysical Research: Atmospheres*, *121*(16), 9342-9355.

Mohsenzadeh Karimi, S., Karimi, S., & Poorrajabali, M. (2018). Forecasting monthly streamflows using heuristic models. *ISH Journal of Hydraulic Engineering*, 1-6.

Mouatadid, S., & Adamowski, J. (2017). Using extreme learning machines for short-term urban water demand forecasting. *Urban water journal*, *14*(6), 630-638.

Napolitano, G., Serinaldi, F., & See, L. (2011). Impact of EMD decomposition and random initialization of weights in ANN hindcasting of daily stream flow series: an empirical examination. *Journal of Hydrology*, *406*(3-4), 199-214.

Quinlan, J. R. (1992, November). Learning with continuous classes. In *5th Australian joint conference on artificial intelligence* (Vol. 92, pp. 343-348).

Rana, G., & Katerji, N. (2000). Measurement and estimation of actual evapotranspiration in the field under Mediterranean climate: a review. *European Journal of agronomy*, *13*(2-3), 125-153.

Rezaie-balf, M., Naganna, S. R., Ghaemi, A., & Deka, P. C. (2017). Wavelet coupled MARS and M5 Model Tree approaches for groundwater level forecasting. *Journal of Hydrology*, *553*, 356-373.

Rezaie-Balf, M., & Kisi, O. (2018). New formulation for forecasting streamflow: evolutionary polynomial regression vs. extreme learning machine. *Hydrology Research*, *49*(3), 939-953.

Rezaie-Balf, M., Kim, S., Fallah, H., & Alaghmand, S. (2019). Daily river flow forecasting using ensemble empirical mode decomposition based heuristic regression models: Application on the perennial rivers in Iran and South Korea. *Journal of Hydrology*, *572*, 470-485.

Sarir, P., Chen, J., Asteris, P. G., Armaghani, D. J., & Tahir, M. M. (2019). Developing GEP tree-based, neuro-swarm, and whale optimization models for evaluation of bearing capacity of concrete-filled steel tube columns. *Engineering with Computers*, 1-19.

Schüttemeyer, D., Schillings, C., Moene, A. F., & De Bruin, H. A. R. (2007). Satellite-based actual evapotranspiration over drying semiarid terrain in West Africa. *Journal of Applied Meteorology and Climatology*, *46*(1), 97-111.

Shiri, J., & Kisi, O. (2010). Short-term and long-term streamflow forecasting using a wavelet and neuro-fuzzy conjunction model. *Journal of Hydrology*, *394*(3-4), 486-493.

Solomatine, D. P., & Dulal, K. N. (2003). Model trees as an alternative to neural networks in rainfall—runoff modelling. *Hydrological Sciences Journal*, *48*(3), 399-411.

Solomatine, D. P., & Xue, Y. (2004). M5 model trees and neural networks: application to flood forecasting in the upper reach of the Huai River in China. *Journal of Hydrologic Engineering*, *9*(6), 491-501.

Sudheer, K. P., Gosain, A. K., Mohana Rangan, D., & Saheb, S. M. (2002). Modelling evaporation using an artificial neural network algorithm. *Hydrological Processes*, *16*(16), 3189-3202.

Talebi, A., Mahjoobi, J., Dastorani, M. T., & Moosavi, V. (2017). Estimation of suspended sediment load using regression trees and model trees approaches (Case study: Hyderabad drainage basin in Iran). *ISH Journal of Hydraulic Engineering*, *23*(2), 212-219.

Trajkovic, S. (2005). Temperature-based approaches for estimating reference evapotranspiration. *Journal of irrigation and drainage engineering*, *131*(4), 316-323.

Wang, W. C., Xu, D. M., Chau, K. W., & Chen, S. (2013). Improved annual rainfall-runoff forecasting using PSO–SVM model based on EEMD. *Journal of Hydroinformatics*, *15*(4), 1377-1390.

Wright, J. L. (1988). Daily and seasonal evapotranspiration and yield of irrigated alfalfa in southern Idaho. *Agronomy Journal*, *80*(4), 662-669.

Wu, Z., & Huang, N. E. (2009). Ensemble empirical mode decomposition: a noise-assisted data analysis method. *Advances in adaptive data analysis*, *1*(01), 1-41.

519 Yeh, J. R., Shieh, J. S., & Huang, N. E. (2010). Complementary ensemble empirical mode
520 decomposition: A novel noise enhanced data analysis method. *Advances in adaptive data*
521 *analysis*, *2*(02), 135-156.
522 Zounemat-Kermani, M., Ramezani-Charmahineh, A., Adamowski, J., & Kisi, O. (2018).
523 Investigating the management performance of disinfection analysis of water distribution
524 networks using data mining approaches. *Environmental monitoring and assessment*, *190*(7),
525 397.
526

527

528

529

530

531

532